Dust acoustic waves in strongly coupled dissipative plasmas

B. S. Xie[1,2,3,*] and M. Y. Yu[4]
[1]*Key Laboratory for Beam Technology and Material Modification at Beijing Normal University, Beijing 100875, China*
[2]*Institute of Low Energy Nuclear Physics, Beijing Normal University, Beijing 100875, China*[†]
[3]*Beijing Radiation Center, Beijing 100875, China*
[4]*Institut für Theoretische Physik I, Ruhr-Universität Bochum, D-44780 Bochum, Germany*
(Received 3 February 2000; revised manuscript received 25 May 2000)

The theory of dust acoustic waves is revisited in the frame of the generalized viscoelastic hydrodynamic theory for highly correlated dusts. Physical processes relevant to many experiments on dusts in plasmas, such as ionization and recombination, dust-charge variation, elastic electron and ion collisions with neutral and charged dust particles, as well as relaxation due to strong dust coupling, are taken into account. These processes can be on similar time scales and are thus important for the conservation of particles and momenta in a self-consistent description of the system. It is shown that the dispersion properties of the dust acoustic waves are determined by a sensitive balance of the effects of strong dust coupling and collisional relaxation. The predictions of the present theory applicable to typical parameters in laboratory strongly coupled dusty plasmas are given and compared with the experiment results. Some possible implications and discrepanies between theory and experiment are also discussed.

PACS number(s): 52.25.Zb, 52.25.Vy, 52.25.Ub, 52.35.Fp

I. INTRODUCTION

Plasmas containing dust particles are of much interest because of their relevance in many space and technological applications [1–3]. In the strongly coupled state the dusts can also form Coulomb crystals that can be easily studied, so that dusty plasmas are also of interest to basic research [4–11]. In the last decade there has been much theoretical and experimental work on the very low frequency dust acoustic waves (DAWs) [12–18], which are dust oscillations driven by the pressure of the electrons and ions. Most existing theories consider the plasma as a collisionless or weakly collisional gaseous system. On the other hand, many experiments are performed in discharges where collisional dissipation and dust correlation are important. Recently, several collisional and other dissipative processes have been studied and found to affect significantly the plasma wave properties [19–23]. Such processes are crucial both in maintaining the equilibrium state of the system and in determining the dispersive/damping properties of the plasma fluctuations. Furthermore, it was found [24–26,28,29] that the DAWs in strongly coupled dust systems can be quite different from that in weakly coupled ones. In particular, negative dispersion can occur when the Coulomb coupling parameter $\Gamma = q_d^2/\delta T_d$ (where $q_d = -Z_d e$ is the charge on the dust grain, δ the interdust distance, and T_d the dust temperature) becomes sufficiently high [25,30]. Moreover, a transverse shear mode can also appear [25,28].

The purpose of the present paper is to reconsider DAW propagation in a plasma containing strongly correlated dusts, accounting for the relevant interactions among the electrons, ions, and dusts. Such a unified study is of interest since dust coupling involves some of the physical parameters governing the dissipative processes. A generalized dispersion relation for the DAWs is derived. The short-relaxation-time hydrodynamic regime and the long-relaxation-time kinetic regime are then analyzed. It is shown that the negative dispersion in the short-wavelength high-dust-correlation regime are enhanced by dissipation. Other new or modified properties such as frequency cutoffs, multiple transitions in the wave dispersion, and enhanced damping are also investigated. The present theory is applicable to typical parameters in laboratory strongly coupled dusty plasmas. As an example, the predictions of DAW wave number with frequency are given and compared with the experiment results [14]. Some possible implication and discrepancies between theory and experiment are also discussed.

II. BASIC EQUATIONS

The average radius a of the dust grains is assumed to be much less than the average intergrain distance δ, the electron (λ_e) and ion (λ_i) Debye radii, as well as the wavelength $2\pi/k$. The dusts satisfy $T_d \ll T_{e,i}$, where $T_{e,i}$ are the temperatures of the electrons and ions, respectively. The charge of a dust grain can vary because of the electron and ion grain currents arising from the potential difference between the dust surface and the adjacent plasma [31].

The equations describing the propagation of DAWs in collisional plasmas with variable dust charge are [19]

$$\partial_t n_e + \nabla(n_e v_e) = -\nu_{ed} n_e + \nu_{\rm ion} n_e - \beta_{\rm eff} n_e^2, \tag{1}$$

$$\nu_e^{\rm eff} v_e + \frac{T_e}{m_e n_e}\partial_x n_e = -\frac{e}{m_e}E, \tag{2}$$

$$\partial_t n_i + \nabla(n_i v_i) = -\nu_{id} n_i + \nu_{\rm ion} n_e - \beta_{\rm eff} n_e^2, \tag{3}$$

$$\nu_i^{\rm eff} v_i + \frac{T_i}{m_i n_i}\partial_x n_i = \frac{e}{m_i}E, \tag{4}$$

*Email address: bsxie@bnu.edu.cn
[†]Mailing address.

where $\nu_{\rm ion}$ is the ionization rate, $\beta_{\rm eff}=\beta-\beta_{si}$, β is the volume recombination rate, and β_{si} is the stepwise ionization rate. The effective frequencies of electron and ion collisions entering Eqs. (2) and (4) are $\nu_e^{\rm eff}=\nu_{ei}+\nu_{en}+\nu_e^{\rm el}+\nu_e^{\rm ch}$, and $\nu_i^{\rm eff}=\nu_{ie}+\nu_{in}+\nu_i^{\rm el}+\nu_i^{\rm ch}$, respectively. Here, ν_{en} and ν_{in} are the rates of electron and ion collisions with the neutrals, and ν_{ei} and ν_{ie} are the rates of electron-ion and ion-electron collisions. The rates of elastic electron- and ion-dust Coulomb collisions are given by $\nu_e^{\rm el}=2\nu_{ed}\Lambda\exp(z)/3$ and $\nu_i^{\rm el}=2\nu_{id}\Lambda/3(\tau+z)\tau$, where $\Lambda=\ln(\lambda_p/a)$ is the Coulomb logarithm and $\lambda_p^2=\lambda_{pe}^{-2}+\lambda_{pi}^{-2}$. In general, the plasma Debye length λ_p satisfies $a\ll\lambda_p$ [33]. For the charging collisions we have [32]

$$\nu_e^{\rm ch}=3\nu_i^{\rm ch}\frac{(4+z)(1+P)(\tau+z)}{4\tau+2z}=\nu_d^{\rm ch}P\frac{\tau+z}{1+\tau+z}\frac{4+z}{z}, \tag{5}$$

where $P=Z_{d0}n_{d0}/n_{e0}$, $\tau=T_i/T_e$, and $z=Z_{d0}e^2/aT_e$. The rates of electron and ion capture by the grain are

$$\nu_{ed}=\frac{n_{i0}}{n_{e0}}\nu_{id}=\nu_d^{\rm ch}\frac{P(\tau+z)}{z(1+\tau+z)}, \tag{6}$$

$$\nu_{id}=\nu_d^{\rm ch}\frac{P(\tau+z)}{z(1+\tau+z)(P+1)}, \tag{7}$$

which have been discussed by many authors [19,21,22,32]. For simplicity, we assume that plasma particle loss is mainly due to volume recombination, and ambipolar diffusion is unimportant, corresponding to intermediate plasma pressures.

For the dust dynamics, we use the generalized viscoelastic hydrodynamic model [5,16,18,25,29] given by

$$\partial_t n_d+\nabla(n_d v_d)=0, \tag{8}$$

$$\mathcal{L}(m_d n_{d0}\partial_t v_d+m_d n_{d0}\nu_{nd}v_d+\nabla P-Z_d e n_{d0}E)=(\zeta+4\eta/3)\nabla^2 v_d, \tag{9}$$

where $\mathcal{L}=1+\tau_m\partial_t$, $\tau_m=\tau_m(k)$ is the relaxation time, and η and ζ are the shear and bulk viscosities, respectively. Furthermore, $\nu_{nd}\approx 4m_n N_n a^2 V_{Tn}/m_d$ is the effective rate of dust-neutral collisions, and m_n, n_n, and V_{Tn} are the mass, density, and thermal velocity of neutrals [17]. The perturbation dust charge $\tilde{q}_d=q_d-q_{d0}$ is governed by the charge balance equation [32]

$$\partial_t\tilde{q}_d+v_d\partial_x\tilde{q}_d+\nu_d^{\rm ch}\tilde{q}_d=-|I_{e0}|\tilde{n}_e/n_{e0}+|I_{i0}|\tilde{n}_i/n_{i0}, \tag{10}$$

where $\nu_d^{\rm ch}=a\omega_{pi}^2(1+\tau+z)/\sqrt{2\pi}V_{Ti}$ is the dust charging rate, $V_{Ti}=(T_i/m_i)^{1/2}$ is the ion thermal speed, ω_{pi} is the ion plasma frequency, and $\tilde{n}_j=n_j-n_{j0}$ is the perturbation particle number density.

The steady-state dust charge is found by equating the equilibrium microscopic electron and ion grain currents I_{e0} and I_{i0} flowing into the dust. These currents arise because of a local potential difference $\Delta\varphi_g$ between the dust surface and the adjacent plasma. Accordingly, for a homogeneous and unmagnetized plasma with thermal ions and electrons we have

$$I_{e0}=-\pi a^2 e(8T_e/\pi m_e)^{1/2}n_{e0}\exp(e\Delta\varphi_g/T_e), \tag{11}$$

$$I_{i0}=\pi a^2 e(8T_i/\pi m_i)^{1/2}n_{i0}(1-e\Delta\varphi_g/T_i), \tag{12}$$

where $\Delta\varphi_g$ is the potential difference between the grain surface and the adjacent plasma.

The system of equations are closed by the Poisson equation

$$\nabla^2\varphi=-4\pi e(n_i-n_e-Z_d n_d), \tag{13}$$

where $E=-\nabla\varphi$ is the electric field of the DAWs, and φ is the electrostatic potential of the waves. For a neutral plasma the charge neutrality condition $n_{i0}=n_{e0}+Z_{d0}n_{d0}$ holds in the equilibrium state.

III. DAW DISPERSION RELATION

From Eqs. (1) and (3) one obtains

$$n_{e0}=(\nu_{\rm ion}-\nu_{ed})/\beta_{\rm eff}\quad\text{and}\quad n_{i0}=(\nu_{ed}/\nu_{id})n_{e0} \tag{14}$$

for the stationary electron and ion densities. Assuming that the wave perturbations behave like $\sim\exp[i(kz-\omega t)]$, linearizing Eqs. (1)–(13) and taking into account Eq. (14) we obtain for the dust charge perturbation,

$$\tilde{Z}_d=-\frac{k^2|I_{e0}|\varphi}{4\pi e^2 n_{e0}\tilde{\nu}_d^{\rm ch}}\left\{\epsilon_{pd}+\frac{Z_{d0}n_{d0}}{n_{i0}\eta_i}\times\left[\omega_{pi}^2-\frac{\nu_i^{\rm eff}(2\nu_{ed}-\nu_{\rm ion})\omega_{pe}^2}{\eta_e}\right]\right\}, \tag{15}$$

where $\tilde{\nu}_d^{\rm ch}=\nu_d^{\rm ch}+\nu_{ed}=\mathcal{B}\nu_d^{\rm ch}$ with $\mathcal{B}=1+P(\tau+z)/z(1+\tau+z)$, $\epsilon_{pd}=1-\omega_{pd}^2/(\omega[\omega+i\{\eta_d(k,\omega)+\nu_{nd}\}]-\gamma_d\mu_d k^2 V_{Td}^2)$ is the dust dielectric function, $\eta_d(k,\omega)=(\zeta+4\eta/3)k^2/m_d n_{d0}(1-i\omega\tau_m)$, γ_d is the adiabatic index, and $\mu_d=(\partial_n P)_T/T_{d0}=1+u(\Gamma)/3+\Gamma\partial_\Gamma u(\Gamma)/9$ is the compressibility [5], and $u(\Gamma)$ is the normalized correlation, or the excess internal, energy of the system. For weakly coupled plasmas ($\Gamma<1$) or strongly coupled plasmas with the Debye-Hückel form for the static structure factor under specific conditions [5,16,29], we have $u(\Gamma)\sim-(\sqrt{3}/2)\Gamma^{3/2}$. In practice, $u(\Gamma)$ is often obtained by fitting data from Monte Carlo or molecular dynamics simulations or experiments. For example, fitting the internal-energy data from a liquid ($1\leqslant\Gamma\leqslant 200$) simulation, one obtains $u(\Gamma)\sim-0.90\Gamma+0.95\Gamma^{1/4}+0.19\Gamma^{-1/4}-0.81+0.01\Gamma/N$, where N is the number of dusts in the system [5]. Other quantities such as the transport coefficients $\zeta(\Gamma)$ and $\eta(\Gamma)$, and the relaxation time $\tau_m(\Gamma)$ can also be so obtained. The forms of the latter can be quite complicated, so that often simplifying models are used [5].

We get from Eqs. (1)–(4):

$$v_e=\frac{ik}{\nu_e^{\rm eff}}\frac{e\varphi}{m_e}-\frac{ikT_e}{m_e\nu_e^{\rm eff}}\frac{\tilde{n}_e}{n_{e0}}, \tag{16}$$

$$\tilde{n}_e=\frac{ek^2 n_{e0}\varphi}{\eta_e m_e}, \tag{17}$$

$$v_i = -\frac{ik}{\nu_i^{\rm eff}}\frac{e\varphi}{m_i} - \frac{ikT_i}{m_i\nu_i^{\rm eff}}\frac{\tilde{n}_i}{n_{i0}}, \tag{18}$$

$$\tilde{n}_i = -\frac{ek^2 n_{i0}\varphi}{\eta_i m_i} + \frac{\nu_i^{\rm eff}(2\nu_{ed}-\nu_{\rm ion})k^2 n_{e0} e\varphi}{\eta_i\eta_e m_e}, \tag{19}$$

where $\eta_e = \nu_e^{\rm eff}(\nu_{\rm ion}-\nu_{ed}) + k^2V_{Te}^2$, $\eta_i = \nu_{id}\nu_i^{\rm eff} + k^2V_{Ti}^2$, and $V_{Te} = \sqrt{T_e/m_e}$. We have assumed $\partial_{Z_d}\nu_{e,i}^{\rm ch} \ll \nu_{e,i}^{\rm ch}$, so that the variations in the rates of electron and ion capture by the dusts arising from the charge fluctuations can be neglected [19].

From the dust conservation laws (8)–(10), we have

$$\tilde{n}_d = -\frac{k^2 n_{d0} e Z_{d0}\varphi/m_d}{\omega[\omega + i(\eta_d(k,\omega)+\nu_{nd})] - \gamma_d\mu_d k^2 V_{Td}^2}, \tag{20}$$

and $\tilde{v}_d = \omega\tilde{n}_d/kn_{d0}$. Substituting Eqs. (15), (17), (19), and (20) into Eq. (13), one obtains the dispersion relation of DAWs in a collisional plasma:

$$\epsilon_{pd} + \frac{\omega_{pe}^2}{\eta_e}\xi_e + \frac{\omega_{pi}^2}{\eta_i}\xi_i = 0, \tag{21}$$

where $\xi_i = \mathcal{B}[1-(Z_{d0}n_{d0}/n_{i0})(\nu_{ed}/\tilde{\nu}_d^{\rm ch})] = (\mathcal{B}+P)/(P+1)$ and $\xi_e = \mathcal{B} - \nu_i^{\rm eff}(2\nu_{ed}-\nu_{\rm ion})\xi_i/\eta_i$. Note that $\xi_i > 1$ since $\mathcal{B} > 1$.

It is convenient to express the relation (21) as

$$\frac{\omega_{pd}^2}{\omega[\omega + i\{\eta_d(k,\omega)+\nu_{nd}\}] - \gamma_d\mu_d k^2 V_{Td}^2} = 1 + \frac{\mathcal{C}}{k^2\lambda_p^2}, \tag{22}$$

where $\mathcal{C} = [\tau\delta_e + (P+1)\delta_i]/(P+1+\tau)$, $\delta_e = k^2V_{Te}^2\xi_e/\eta_e$, and $\delta_i = k^2V_{Ti}^2\xi_i/\eta_i$. For many dusty plasmas we have $\tau \ll 1$ and $\tau\delta_e < (P+1)\delta_i$, so that one can write

$$\mathcal{C} \sim \xi_i\frac{k^2\lambda_p^2}{k^2\lambda_p^2 + \mathcal{R}},$$

where we have ignored the electron contribution to λ_p, so that $\mathcal{C} \sim \delta_i$ and $\mathcal{R} = \nu_{id}\nu_i^{\rm eff}/\omega_{pi}^2$ represents effective dissipation. In many earlier studies, the weak-collision limit $\mathcal{C}=1$ was considered [25,26]. Here we are interested in collisional plasmas that are typical for laboratory studies of dusts in plasmas.

Normalizing all the time and space quantities by the inverse dust plasma frequency ω_{pd}^{-1} and the average interdust distance δ, respectively, and introducing $\eta^* = (\zeta + 4\eta/3)/m_d n_{d0}\omega_{pd}\delta^2$, $\kappa = \delta/\lambda_p$, one obtains for the generalized DAW dispersion relation:

$$\omega(\omega + i\nu_{nd}) - \gamma_d\mu_d k^2\lambda_d^2 + i\omega k^2\eta^*/(1 - i\omega\tau_m) = (1 + \mathcal{C}\kappa^2/k^2)^{-1}, \tag{23}$$

where ω, k, τ_m, ν_{nd}, etc. are now dimensionless, and the dimensionless parameter $\mathcal{C}$ can be written as

$$\mathcal{C} \sim \frac{k^2}{k^2 + \mathcal{R}\kappa^2},$$

where we have used $\xi_i \sim 1$. The argument for this approximation is threefold: first, for $P \ll 1$, we have $\mathcal{B} \sim 1$, so that $\xi_i = (B+P)/(P+1) \sim 1$; second, for $P \sim O(1)$, we have $\mathcal{B} \sim 1 + P/(z+1) \sim O(1)$, so that $\xi_i = (B+P)/(P+1) \sim 1$; and third, for $P \gg 1$, we have $\mathcal{B} \sim P/(z+1) \sim O(P)$ since $z \sim O(1)$, so that $\xi_i = (B+P)/(P+1) \sim 2$ and without loss of generality we can use $\xi_i \sim 1$.

The quantities η^* and τ_m clearly play important roles in the dynamics of DAWs in dissipative plasmas with strongly coupled dusts. In certain parameter ranges it is possible to construct approximate expressions from simulations, experiments, or simple theoretical models. For our purpose, we obtain from Table 5 and Fig. 33 of Ref. [5]

$$\eta^* \sim 0.02\sqrt{\Gamma}, \tag{24}$$

which is from the one-component-plasma model and is valid for $10 \leqslant \Gamma \leqslant 200$.

Writing $\omega = \omega_r + i\omega_i$, we get from Eq. (23) the coupled equations

$$2\omega_i + \nu_d^{\rm eff} + \frac{k^2\eta^*}{(1+\tau_m\omega_i)^2 + (\tau_m\omega_r)^2} = 0, \tag{25}$$

$$[1 + \tau_m(2\omega_i + \nu_d^{\rm eff})](\omega_r^2 + \omega_i^2) = \mathcal{D}, \tag{26}$$

for the DAW frequency ω_r and the damping rate ω_i. We have introduced the dimensionless quantity $\mathcal{D} = \gamma_d\mu_d k^2\lambda_d^2 + (k^2 + \mathcal{R}\kappa^2)/[k^2 + (1+\mathcal{R})\kappa^2]$.

To complete the equations, the k dependence of τ_m is needed. One can write [5]

$$\tau_m(k) = \tau_m(0)Y(k), \tag{27}$$

where $\tau_m(0) = (\eta^*/\lambda_d^2)[1 - \gamma_d\mu_d + 4u(\Gamma)/15]^{-1}$. Assuming a Gaussian distribution for k with the scaling k^*, we have $Y(k) = \exp[-(k/k^*)^2]$. Thus, $\tau_m(k)$ decreases rapidly with k. However, for numerical work it is often convenient [5] to use the Lorentzian distribution $Y(k) = [1 + (k/k^*)^2]^{-1}$.

IV. NUMERICAL RESULTS

For the regime of strong dust coupling, Kaw and Sen investigated both the hydrodynamic ($|\omega_r|\tau_m \ll 1$) and kinetic ($|\omega_r|\tau_m \gg 1$) limits [25] without including dissipative and charging processes ($\mathcal{R}=0$ and $\mathcal{C}=1$). We shall present here a more complete picture solving Eqs. (25) and (26) exactly. Accordingly, we obtain

$$\mathcal{F}^3 - (1+\tau_m\nu_{nd})\mathcal{F}^2 + \mathcal{G}\mathcal{F} - \tau_m^2\mathcal{D} = 0, \tag{28}$$

$$\omega_i = -\frac{1}{2}\left(\nu_{nd} + \frac{1-\mathcal{F}}{\tau_m}\right), \tag{29}$$

$$\omega_r^2 = \mathcal{D}/\mathcal{F} - \omega_i^2, \tag{30}$$

where $\mathcal{F} = 1 + \tau_m(2\omega_i + \nu_{nd})$ and $\mathcal{G} = \tau_m^2\mathcal{D} + \tau_m k^2\eta^* + \tau_m\nu_{nd}$. Since $\mathcal{D}$ may be negative for strong coupling, there is a lower cutoff for k in certain cases.

The properties of the DAWs in the strongly coupled regime can be made clearer by numerically evaluating Eqs. (28), (29), and (30). In Figs. 1–4 we show the DAW fre-

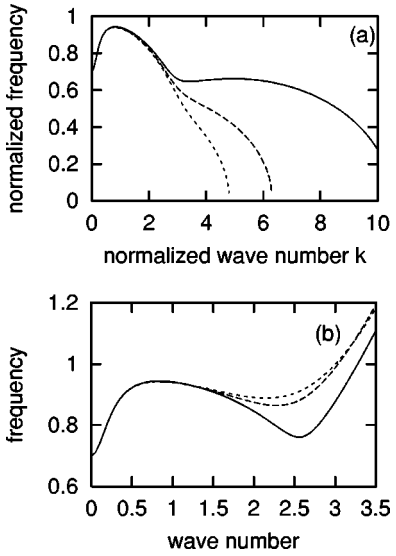

FIG. 1. The real normalized frequency ω_r/ω_{pd} versus the normalized wave number $k\delta$ for $\Gamma=20$ (solid line), 60 (long-dashed line), and 200 (short-dashed line) at $\kappa=0.2$, $\nu_{nd}=0.2$, and $\mathcal{R}=1$ for (a) constant τ_m, and (b) k-dependent τ_m.

quency ω_r versus k for different values of the coupling parameter Γ, the ratio κ of the average interdust distance to the plasma Debye length, the dust-neutral collision frequency ν_{nd}, and the effective plasma dissipative parameter $\mathcal{R}$, respectively. Without loss of generality we ignore the contribution of the electrons to $\mathcal{C}$ and $\mathcal{R}$.

In Fig. 1, we plot the DAW frequency ω_r versus the wave vector k for $\Gamma=20$, 60, and 200, at $\kappa=0.2$, $\nu_{nd}=0.2$, and $\mathcal{R}=1$. We see that the effect of Γ on the DAW frequency is strongest in the short wavelength regime and there is almost no effect for $k\leqslant 1$. Multiple transition behavior in the DAW dispersion at higher k values usually appears. For constant τ_m [Fig. 1(a)], we see that the first transition, a local frequency maximum at $\omega=\omega_{r,\max 1}$, occurs at $k=k_{1c}\sim 0.8$, and $\omega_{r,\max 1}$ decreases with Γ. The second and third transitions, appearing at larger k values as a local frequency minimum and maximum, respectively, vanish for large Γ. When the relaxation time is k-dependent [Fig. 1(b)], the transitions in the DAW dispersion tend to disappear since τ_m and its effect vanishes rapidly as k increases.

In Fig. 2, we plot ω_r versus k for $\kappa=0.2$, 0.8, and 2.0 with $\Gamma=20$, $\nu_{nd}=0.2$, and $\mathcal{R}=1$. Here, we see that the DAW dispersion depends strongly on κ at all wavelengths except for $k\rightarrow\infty$. As κ is increased, the first transition (a local frequency maximum) occurs at lower frequencies and eventually disappears, so that there is a fundamental change in the dispersion properties of the DAWs at long wavelengths. Again, the second peak in the dispersion curve does not exist if the relaxation time is k-dependent, and the DAWs at large k behave very differently for k-dependent and -independent relaxation times.

In Fig. 3 we plot ω_r versus k for $\nu_{nd}=0$,0.2 and 0.8 for $\Gamma=20$, $\kappa=0.2$, and $\mathcal{R}=1$. Here, the DAW dispersion is

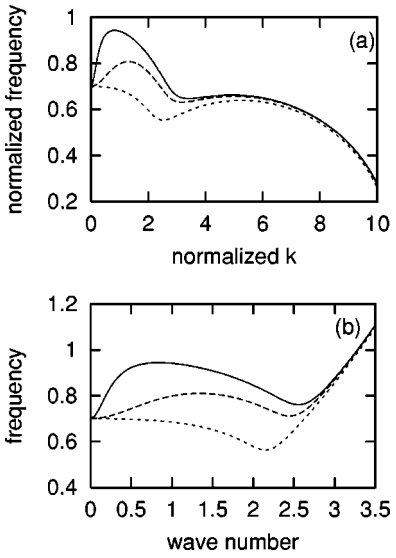

FIG. 2. Same as in Fig. 1, but for $\kappa=$ 0.2 (solid line), 0.8 (long-dashed line), and 2.0 (short-dashed line) at $\Gamma=20$.

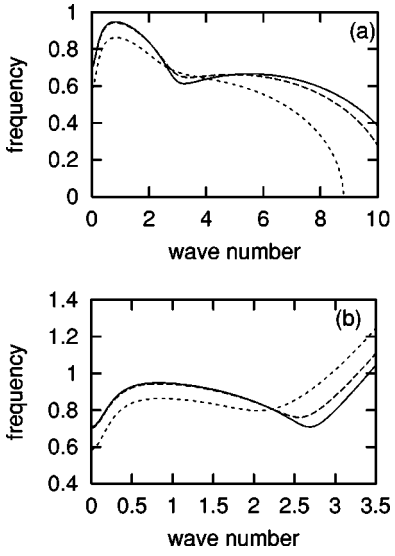

FIG. 3. Same as in Fig. 1, but for $\nu_{nd}=0$ (solid line), 0.2 (long-dashed line), and 0.8 (short-dashed line), at $\Gamma=20$.

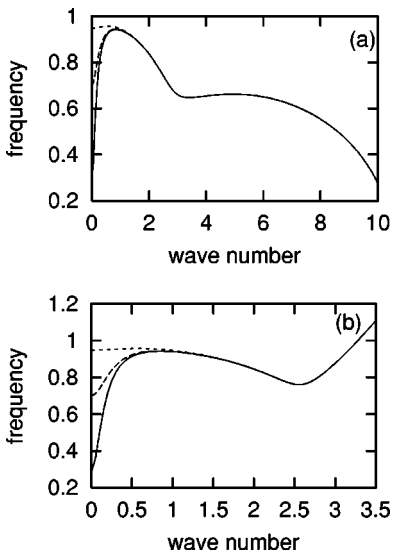

FIG. 4. Same as in Fig. 1, but for $\mathcal{R}=$ 0.1 (solid line), 1.0 (long-dashed line), and 10 (short-dashed line) at $\Gamma=20$.

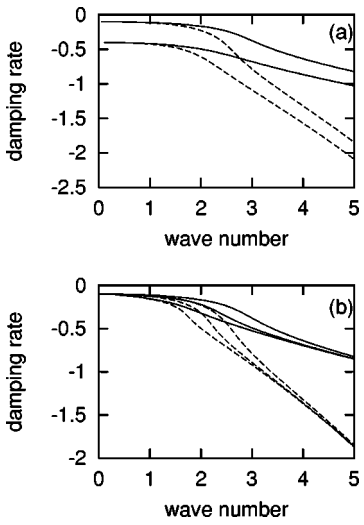

FIG. 5. The normalized damping rate ω_i/ω_{pd} versus the wave vector $k\delta$ for (a) $\Gamma=20$, $\kappa=0.2$, and $\mathcal{R}=0.01$ for $\nu_{nd}=0.2$ (upper lines) and 0.8 (lower lines); (b) $\Gamma=20$, $\kappa=2$, and $\nu_{nd}=0.2$ for $\mathcal{R}=0.01$, 1.0, and 100 (lines from bottom to top). The solid and dashed curves are for *k*-independent and *k*-dependent τ_m, respectively.

strongly dependent on ν_{nd} at all wavelengths. Otherwise the dispersion behavior is similar to that for the *k*-dependent τ_m case, there is again only one local frequency maximum. It decreases with ν_{nd} and occurs at smaller *k* values. The back transition frequency $\omega_{r,\min}$ increases with ν_{nd} and occurs at smaller *k* values. The transitions tend to vanish as ν_{nd} becomes sufficiently large.

In Fig. 4, we present ω_r versus *k* for $\mathcal{R}=0.1$, 1.0, and 10 at $\Gamma=20$, $\kappa=0.2$, and $\nu_{nd}=0.2$. We see that the dissipation parameter $\mathcal{R}$ plays an important role on the DAW dispersion only for $k<1$. It has almost no effect on shorter-wavelength DAWs. For small $\mathcal{R}$, the result approaches that for $C=1$, when electron and ion capture by the dusts as well as collisions can be ignored. In this case the long-wavelength DAW dispersion relation becomes the same as that ($\omega_r\sim kc_d$, where c_d is the dust-acoustic speed) of the classical DAWs. On the other hand, as $\mathcal{R}$ increases, the DAW frequency cutoff (at $k\to 0$) $\omega=\omega_c$ also increases and approaches the dust plasma frequency ($\omega_c\sim 1$). This is not surprising since for large dissipation ($\mathcal{R}\gg 1$) the right-hand side of Eq. (22) is nearly unity, so that the coupling of the dusts to the electrons and ions is lost, and only characteristic dust oscillations remain.

In Fig. 5, we present the imaginary part ω_i of the DAW frequency versus the wavelength *k* for several parameter values used in Figs. 1–4. We see that for small κ one can hardly distinguish the damping rates for $\mathcal{R}=0.01$,1.0,100. However, when κ is increased ($\kappa=2$), differences among the damping rates appear. We also see that the *R* dependence of the damping rate is weak for both small and large *k* values.

Numerically, one can show that in general the parameter *q* decreases from 1 at $k=0$ to a (negative) minimum value at some *k*, and then increases to 0 at $k\to\infty$. Therefore in the regime of small *k* the damping of DAWs is mainly determined by dust-neutral collisions. Furthermore, the *k* dependence of the relaxation time also greatly enhances the damping of short-wavelength DAWs.

V. DISCUSSION

It is necessary to determine the physically relevant values of $\mathcal{R}\sim\nu_{id}\nu_i^{\rm eff}/\omega_{pi}^2$, representing the relative importance of the ion-dust charging collision and the effective ion collisions with the other particles. For typical gas discharge plasmas, say argon at intermediate pressures with $T_e=1$ eV, $T_i=0.1$ eV, and $N_n\sim 5\times 10^{15}$ cm^{-3}, and assuming $\sigma_{en}\sim 1.5\times 10^{-16}$ cm^{-3} and $\sigma_{in}\sim 3\times 10^{-15}$ cm^{-3} [21,22], we obtain $\nu_{en}\sim 1.8\times 10^7$ s^{-1} and $\nu_{in}\sim 4.2\times 10^5$ s^{-1}. Further assuming that $n_{i0}\sim 10^{10}$ cm^{-3} and $n_{e0}\sim 0.5n_{i0}$, one obtains for the electron-ion and ion-electron collision rates $\nu_{ei}\sim 10^5$ s^{-1} and $\nu_{ie}\sim 2\times 10^4$ s^{-1}. The ion plasma frequency is $\omega_{pi}\sim 2\times 10^7$ s^{-1}. Thus $\tau\equiv T_i/T_e=0.1$, $P\equiv Z_{d0}n_{d0}/n_{e0}=1$, $z\sim 3$, $\mathcal{B}\sim 1.25$, $\xi_i\sim 1$. From the dust charging rate $\nu_d^{\rm ch}=a\omega_{pi}^2(1+\tau+z)/\sqrt{2\pi}V_{Ti}$, one can obtain $\nu_d^{\rm ch}\sim 10^7 a$, where *a* is the dust size in micrometers. Thus, $\nu_i^{\rm ch}\sim 10^6 a$, $\nu_i^{\rm el}\sim 10^7 a$, so that $\nu_i^{\rm eff}=\nu_{ie}+\nu_{in}+\nu_i^{\rm el}+\nu_i^{\rm ch}\sim\nu_i^{\rm el}\sim 10^7 a$ for $a\geq 0.1$ μm. Note that $\nu_{id}\sim 10^6 a$, so that $\mathcal{R}\equiv\nu_{id}\nu_i^{\rm eff}/\xi_i\omega_{pi}^2\sim a^2/40$. It follows that the values $\mathcal{R}=0.1$,1.0, and 10 in our numerical calculations correspond to, for example, $a\sim 2$,6, and 20 μm, respectively. It should also be mentioned that we have neglected the variation of the electron and ion capture (by the dusts) rates arising from wave-induced fluctuations in the average dust charge, and this assumption may not be applicable for larger dust particles and higher ion densities [22]. For example, for $n_{i0}\sim 10^{10}$ cm^{-3} and $Z_{d0}\sim 5000$, a dust size of $a\leq 100$ μm would be required, corresponding to $\mathcal{R}_{\max}\sim 250$.

It is of interest to compare our results with that of existing experiments and weak-coupling theories. For convenience, we shall compare with the work of Pieper and Goree [14] and use their experimental parameter values. Although their experiment was under strong-dust-coupling conditions, the DAW dispersion relation from a weak-coupling theory as given by Eq. (2) of Ref. [14] seems to fit the experiment data very well. This striking observation leads to many arguments and discussions invoking mechanisms such as dust shielding [16,29], the effect of κ [14,27], the competition and transition between the longitudinal DAWs and the dust lattice waves (DLWs), or between the transverse shear waves and the DLWs [27,28], etc. For the purpose of comparison, we rewrite the generalized DAW dispersion relation Eq. (23) as

$$k^2=\frac{1}{\mathcal{H}-\omega(\omega+i\nu_{nd})}-(\mathcal{R}+1), \tag{31}$$

where

$$\mathcal{H}=1-\left(\frac{i\omega\eta^*}{1-i\omega\tau_m}-\gamma_d\mu_d\lambda_d^2\right)\kappa^2k^2, \tag{32}$$

and *k* is now normalized by $k_D=1/\lambda_p$. The dispersion relation (31) is in a form similar to Eq. (2) of Ref. [14]. In the limit $\mathcal{H}=1$ and $\mathcal{R}=0$, Eq. (31) reduces to the latter.

We solve the dispersion relation (31) numerically and the results are given in Fig. 6, which corresponds to Fig. 2 of [14]. The corresponding value of the dissipative parameter $\mathcal{R}$ was estimated as follows. It is found that $Z_{d0}n_{d0}\sim 10^{7-8}$, $\omega_{pi}\sim 10^{8-9}$, $\nu_{id}\sim 10^{0-1}\nu_d^{\rm ch}\sim 10^{6-7}$ for $P\gtrsim 1$, $a\sim 1$ μm and $\lambda_p\sim 1$ mm (note that our λ_p is λ_D in [14]). Furthermore,

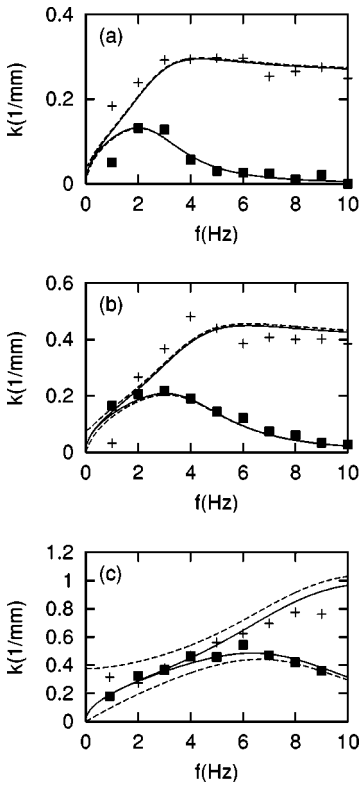

FIG. 6. The real (k_r) and imaginary (k_i) wave vector versus the frequency $f=\omega/2\pi$ from Eq. (2) of Ref. [14] (solid line), and from Eq. (31) here (dashed line, note that the parameters are dimensional). The squares and + 's are from the experimental data of Ref. [14] for k_r and k_i, respectively. (a) $\Gamma=32$, $\kappa=0.15$, $\omega_{pd}/2\pi=3.2$, $\nu_{nd}=1.22$, $\lambda_p=3.85$ mm, and $\mathcal{R}=0.021$; (b) $\Gamma=11.4$, $\kappa=0.18$, $\omega_{pd}/2\pi=4.6$, $\nu_{nd}=1.13$, $\lambda_p=2.56$ mm, and $\mathcal{R}=0.040$; (c) $\Gamma=2400$, $\kappa=0.24$, $\omega_{pd}/2\pi=9.0$, $\nu_{nd}=1.00$, $\lambda_p=1.19$ mm, and $\mathcal{R}=0.20$.

since $\nu_i^{\rm eff}\sim\nu_i^{\rm el}\sim 10^{1-2}\nu_{id}\sim 10^{7-9}$ for $\tau\lesssim 1$, we obtain $\mathcal{R}\sim 10^{-3}$ to unity. For typical gas discharges $\tau\ll 1$, and we assume that this is also valid in Ref. [14]. Since most electrons participate in charging the dusts, we have $P\gtrsim 1$. Therefore we obtain for the maximum value of $\mathcal{R}$:

$$\mathcal{R}_{\rm max}\sim 1.6\times 10^{-3}\left(\frac{a[\mu{\rm m}]}{z\lambda_D[{\rm mm}]}\right)^2,$$

where $P=10$ and $z=Z_{d0}e^2/aT_e$. For $\tau\sim 0.1$, we have $z\sim 0.18,0.20,0.19,0.96$ and $\mathcal{R}_{\rm max}\sim 0.021,0.040,0.20,0.19$, corresponding to the experiments shown in Fig. 2 of Ref. [14], respectively.

In Fig. 6, we also show the results from the weak-coupling theory and the experiments [14]. Figures 6(a) and 6(b) show that the difference between the results of our Eq. (31) and that of the Eq. (2) of Ref. [14] is hardly distinguishable. This is because at low dissipation ($\mathcal{R}\ll 1$) and small κ, moderate coupling ($\Gamma\lesssim 32$) introduces little modification to the classical DAW dispersion. However, for high $\Gamma\gtrsim 2400$ the difference between the weak and strong coupling theories is evident. Furthermore, the strong-coupling theory seems to agree better with the experimental results at low frequencies. In particular, there always exists a purely damped mode when the frequency vanishes. On the other hand, for $\Gamma\gtrsim 2400$ the validity of Eq. (24) may be violated. We did not make a comparison for a case corresponding to Fig. 2(d) in [14] since there the Γ value is too high for our fluid theory to be valid.

In conclusion, using the viscoelastic hydrodynamic theory with finite relaxation time, we have investigated longitudinal DAWs in a collisional plasma with highly correlated dusts. A generalized formula for the DAW dispersion relation including the hydrodynamic as well as the kinetic regimes is obtained. It is shown that accounting for ionization and recombination, dust charging, as well as dust relaxation results in a modification of the dispersion and damping properties of the DAWs. It is also shown that competing parameters such as the Coulomb coupling parameter, the ratio of the interdust distance to the plasma Debye radius, and the dust-neutral collisional frequency strongly affect the behavior of the DAWs. The competition of these parameters may also explain why weak-coupling theories seem to work for strongly coupled dust systems. Furthermore, the multiple transitions found in the wave dispersion depend sensitively on these parameters. It is expected that the phenomena observed here can also occur for the newly discovered transverse mode [25,26,28] in strongly coupled dissipative dusty plasmas.

ACKNOWLEDGMENTS

This work was supported by the National Natural Science Foundation of China (NSFC) under Grant No. 19905001, the Special Funds for Major State Basic Research Project of China, and partially by the Sonderforschungsbereich 191 Niedertemperatur Plasmen.

[1] C.K. Goertz, Rev. Geophys. **27**, 271 (1989).
[2] G.S. Selwyn, Jpn. J. Appl. Phys., Part 1 **32**, 3068 (1993).
[3] A. Bouchoule and L. Boufendi, Plasma Sources Sci. Technol. **3**, 262 (1994).
[4] H. Ikezi, Phys. Fluids **29**, 1764 (1986).
[5] See, for example, S. Ichimaru, Rev. Mod. Phys. **54**, 1017 (1982); S. Ichimaru and S. Tanaka, Phys. Rev. Lett. **56**, 2815 (1986); S. Tanaka and S. Ichimaru, Phys. Rev. A **35**, 4743 (1987); S. Ichimaru, H. Iyetomi, and S. Tanaka, Phys. Rep. **149**, 91 (1987).
[6] J.H. Chu and Lin I, Phys. Rev. Lett. **72**, 4009 (1994); Lin I, W.T. Juan, C.H. Chiang, and J.H. Chu, Science **272**, 1626 (1996); W.T. Juan and Lin I, Phys. Rev. Lett. **80**, 3073 (1998).
[7] H. Thomas, G.E. Morfill, V. Demmel, J. Goree, B. Feuerbacher, and D. Mohlmann, Phys. Rev. Lett. **73**, 652 (1994).
[8] R.A. Quinn, C. Cui, J. Goree, J.B. Pieper, H. Thomas, and G.E. Morfill, Phys. Rev. E **53**, R2049 (1996).
[9] S. Nunomura, N. Ohno, and S. Takamura, Phys. Plasmas **5**, 3517 (1998).
[10] V.N. Tsytovich and J. Winter, Usp. Fiz. Nauk. **168**, 899 (1998).
[11] W.T. Juan, Z.H. Huang, J.W. Hsu, Y.J. Lai, and Lin I, Phys. Rev. E **58**, R6947 (1998).

[12] N.N. Rao, P.K. Shukla, and M.Y. Yu, Planet. Space Sci. **38**, 543 (1990).
[13] A. Barkan, R.L. Merlino, and N. D'Angelo, Phys. Plasmas **2**, 3563 (1995).
[14] J.B. Pieper and J. Goree, Phys. Rev. Lett. **77**, 3137 (1996).
[15] R.L. Merlino, A. Barkan, C. Thompson, and N. D'Angelo, Phys. Plasmas **5**, 1607 (1998).
[16] X. Wang and A. Bhattacharjee, Phys. Plasmas **3**, 1189 (1996); **4**, 3759 (1997).
[17] N. D'Angelo, Phys. Plasmas **5**, 3155 (1998).
[18] B.S. Xie, K.F. He, and Z.Q. Huang, Phys. Plasmas **6**, 3808 (1999).
[19] K.N. Ostrikov, M.Y. Yu, S.V. Vladimirov, and O. Ishihara, Phys. Plasmas **6**, 737 (1999).
[20] A.V. Ivlev, D. Samsonov, J. Goree, and G. Morfill, Phys. Plasmas **6**, 741 (1999).
[21] S.V. Vladimirov, K.N. Ostrikov, and M.Y. Yu, Phys. Rev. E **60**, 3257 (1999).
[22] K.N. Ostrikov, S.V. Vladimirov, M.Y. Yu, and G.E. Morfill, Phys. Plasmas **7**, 461 (2000).
[23] A.V. Ivlev and G. Morfill, Phys. Plasmas **5**, 1094 (2000).
[24] M. Rosenberg and G. Kalman, Phys. Rev. E **56**, 7166 (1997).
[25] P.K. Kaw and A. Sen, Phys. Plasmas **6**, 3552 (1998).
[26] M.S. Murillo, Phys. Plasmas **5**, 3116 (1998).
[27] N.F. Otani, A. Bhattacharjee, and X. Wang, Phys. Plasmas **6**, 409 (1999).
[28] X. Wang and A. Bhattacharjee, Phys. Plasmas **6**, 4388 (1999).
[29] B.S. Xie, K.F. He, Z.Q. Huang, and M.Y. Yu, Phys. Plasmas **6**, 2997 (1999).
[30] B.S. Xie and M.Y. Yu, Phys. Plasmas **7**, 3137 (2000).
[31] F. F. Chen, in *Plasma Diagnostic Techniques*, edited by R. H. Huddlestone and S. L. Leonard (Academic, New York, 1965), Chap. 4.
[32] V.N. Tsytovich, Usp. Fiz. Nauk **40**, 53 (1997) [Phys. Usp. **40**, 53 (1997)], and the references therein.
[33] E. W. McDaniel, *Collision Phenomena in Ionized Gases* (Wiley, New York, 1964); L. M. Biberman, V. S. Vorob'ev, and I. T. Yakubov, *Kinetics of Non-Equilibrium Low-Temperature Plasmas* (Nauka, Moscow, 1982).